

**Supplemental information**

**Met/HGFR triggers detrimental  
reactive microglia in TBI**

**Rida Rehman, Michael Miller, Sruthi Sankari Krishnamurthy, Jacob Kjell, Lobna Elsayed, Stefanie M. Hauck, Florian olde Heuvel, Alison Conquest, Akila Chandrasekar, Albert Ludolph, Tobias Boeckers, Medhanie A. Mulaw, Magdalena Goetz, Maria Cristina Morganti-Kossmann, Aya Takeoka, and Francesco Roselli**

## **Supplemental information**

### **Met/HGFR triggers detrimental reactive microglia in TBI**

Rida Rehman, Michael Miller, Sruthi Sankari Krishnamurthy, Jacob Kjell, Lobna Elsayed, Stefanie M. Hauck, Florian olde Heuvel, Alison Conquest, Akila Chandrasekar, Albert Ludolph, Tobias Boeckers, Medhanie A Mulaw, Magdalena Goetz, Maria Cristina Morganti-Kossmann, Aya Takeoka, and Francesco Roselli

**Figure S1. Neuronal survival and RTK phosphorylation over time post TBI. Related to Figure 1.**

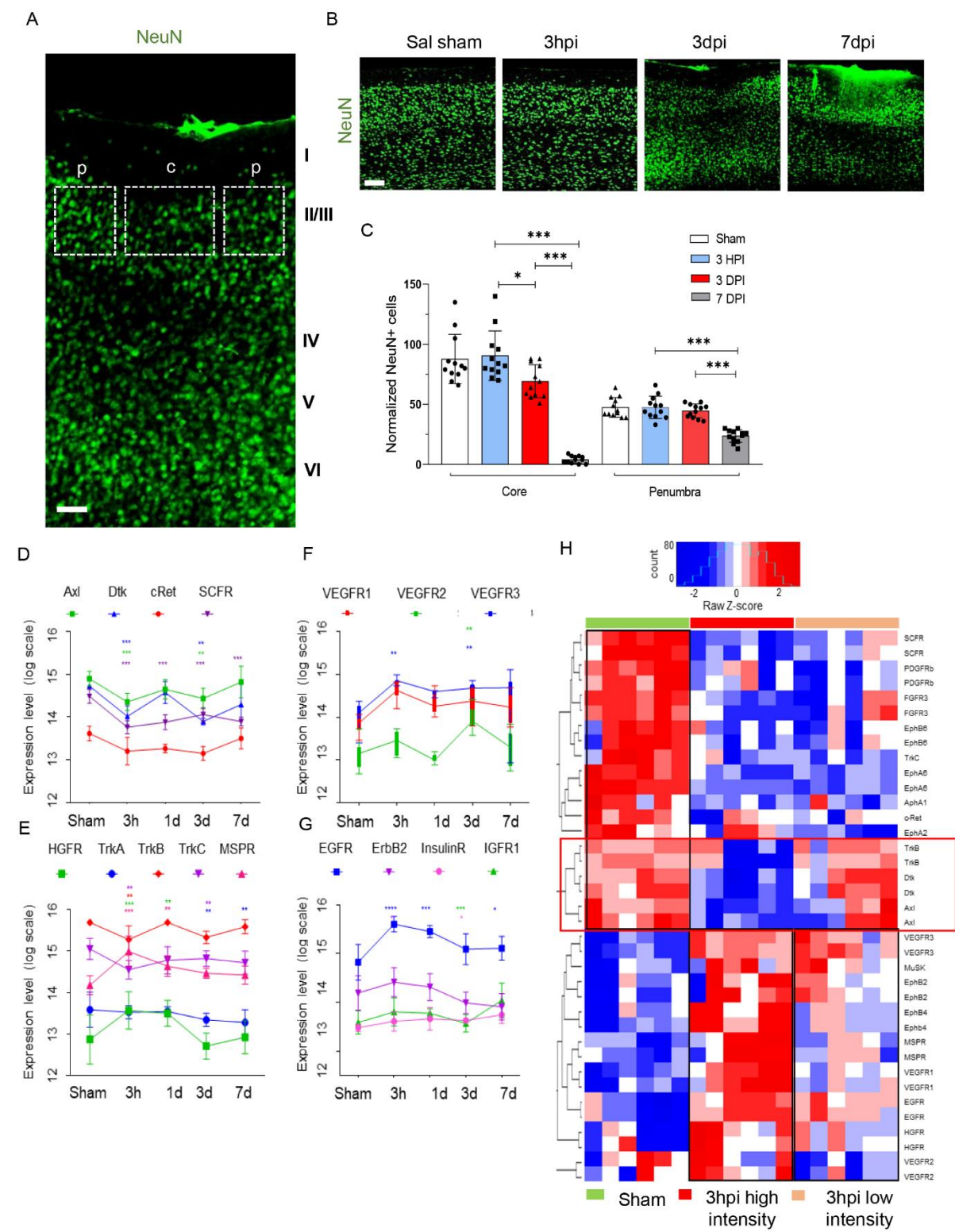


**Figure S1. Neuronal survival and RTK phosphorylation over time post TBI. Related to Figure 1.**

**(A)** Position of Region of Interest (ROI) in the imaged brain section to display injury core (c) and surrounding penumbra (p) in layer II/III. **(B)** Immunolabeling of neurons (NeuN, green) at sham, 3 hpi, 1 dpi, 3 dpi and 7 dpi to ascertain the impact elicited by weight-drop trauma model. **(C)** The histogram displayed the number of neurons significantly decreasing at 7DPI. **(D-G)** Graphs displayed the expression pattern of individual proteins over time. **(H)** Comparison of RTK phosphorylation pattern between two different intensities of trauma.

All graphs were represented as mean  $\pm$  SD. In **(B-C)**, n=4 for sham, 3 hpi, 3 dpi and 7 dpi. Dots, squares and triangles indicate the number of cells/section and four sections/animal. Significance of differences between means were analyzed using one-way ANOVA test with bonferroni correction. (\*p<0.05, \*\*p<0.05, \*\*\*p<0.0001). In **(D-H)**, n=6 for sham, 1 dpi, 3 hpi low intensity, 3 dpi and 7 dpi and n=7 for 3 hpi high intensity. Significance for DE proteins was set at P<0.05 (FDR adjusted). Scale bars: 200 $\mu$ m and 300 $\mu$ m for **(A)** and **(B)**, respectively. Statistical analysis is based on the number of animals per group. Detailed individual comparisons between respective groups and the overlapping phosphorylation pattern for the proteins shown in Data S1.

**Figure S2. Cell specific expression of pMet, pBtk and pVEGFR1. Related to Figure 2.**

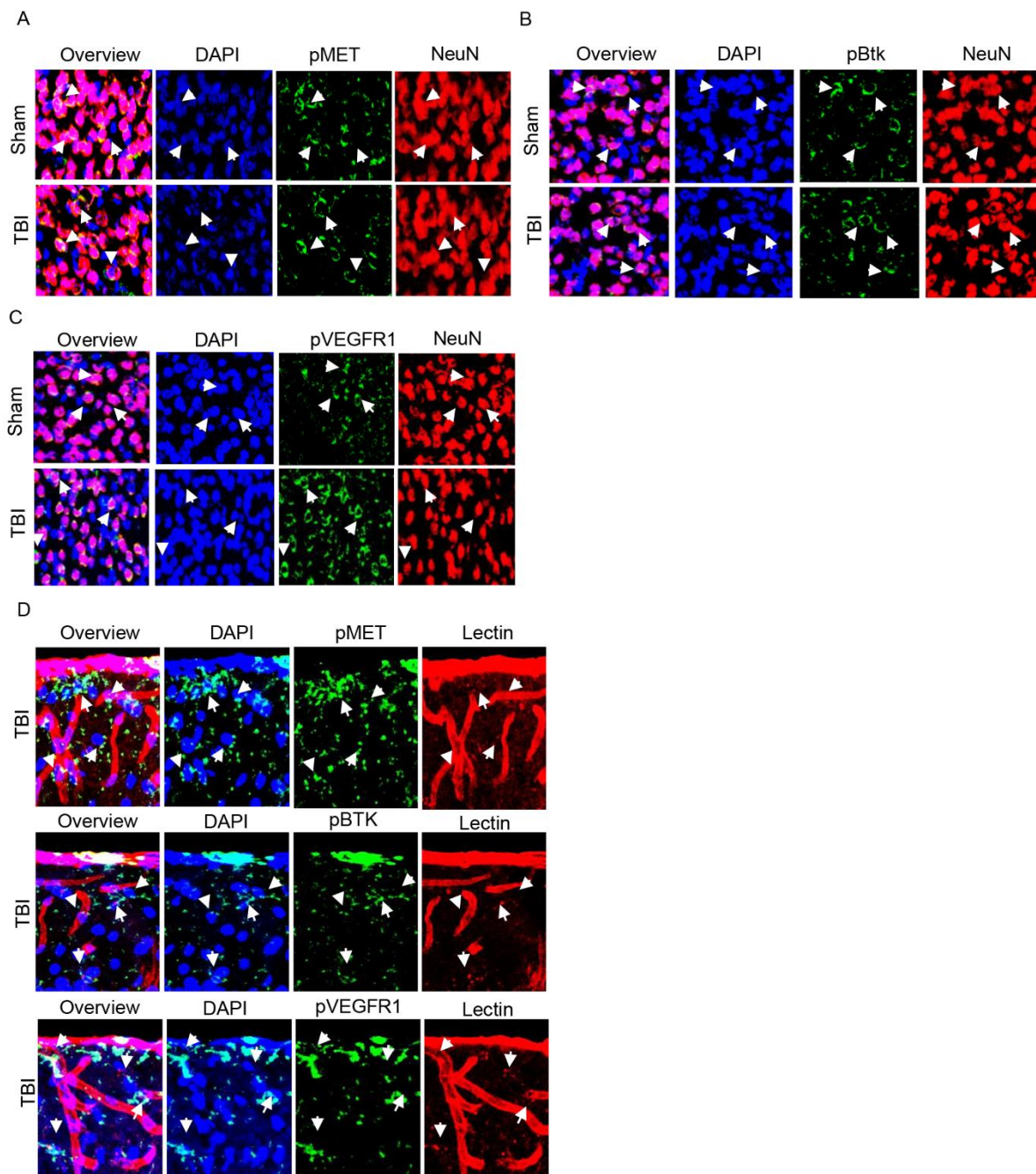


**Figure S2. Cell specific expression of pMet, pBtk and pVEGFR1. Related to Figure 2.** (A-C) Immunostaining was performed to identify neuronal expression of (A) pMet, (B) pBtk and (C) pVEGFR1. No significant difference in pMet and pBtk levels was observed in neurons post trauma however pVEGFR1 levels were elevated in neurons after trauma. (D) Vascular co-staining showed no overlap between pMet, pBtk, but slight overlap in pVEGFR1 expression.

**Figure S3**

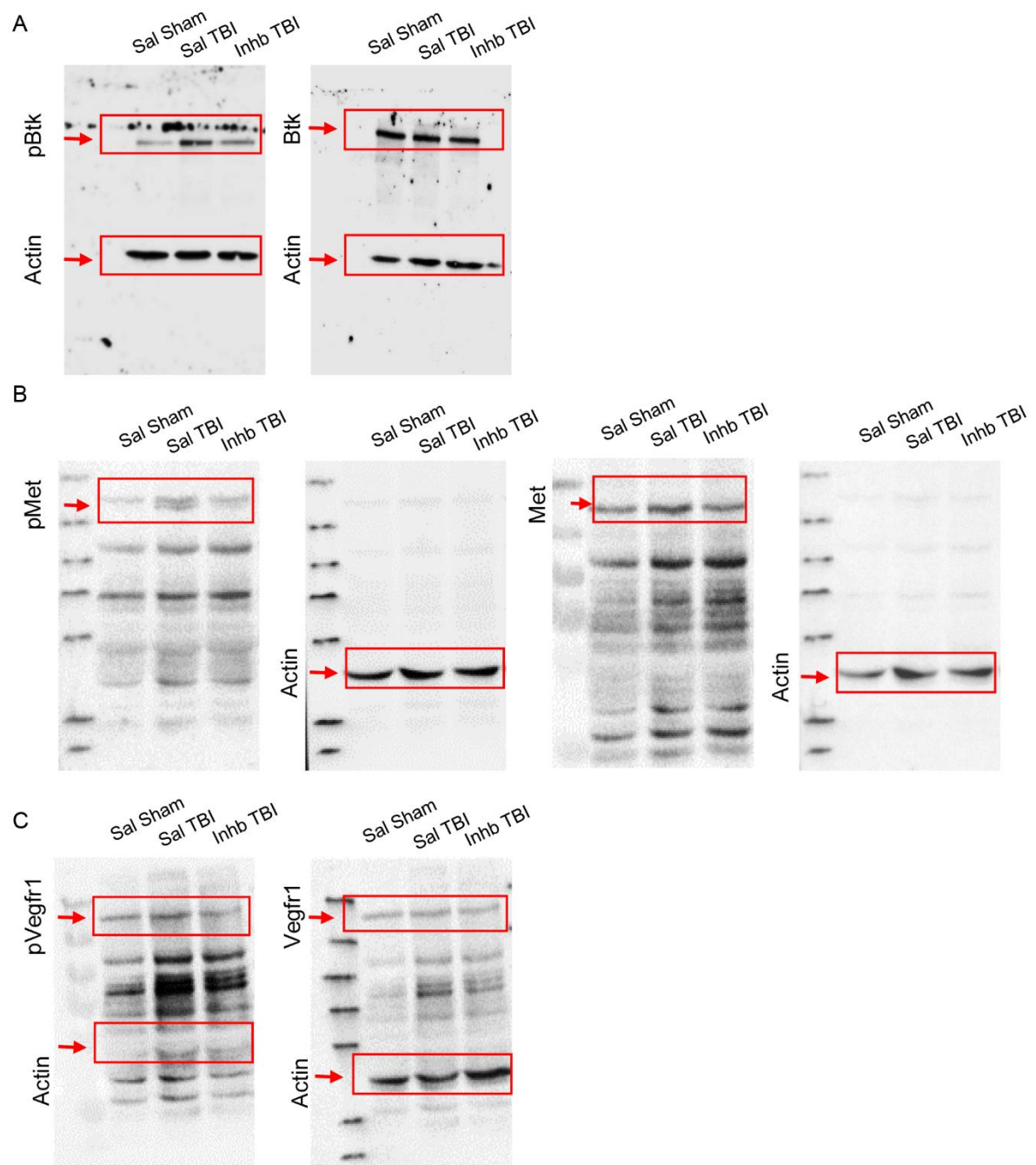


**Figure S3. Full scans of western blots data. Related to Figure 3B-D.**



**Figure S4**

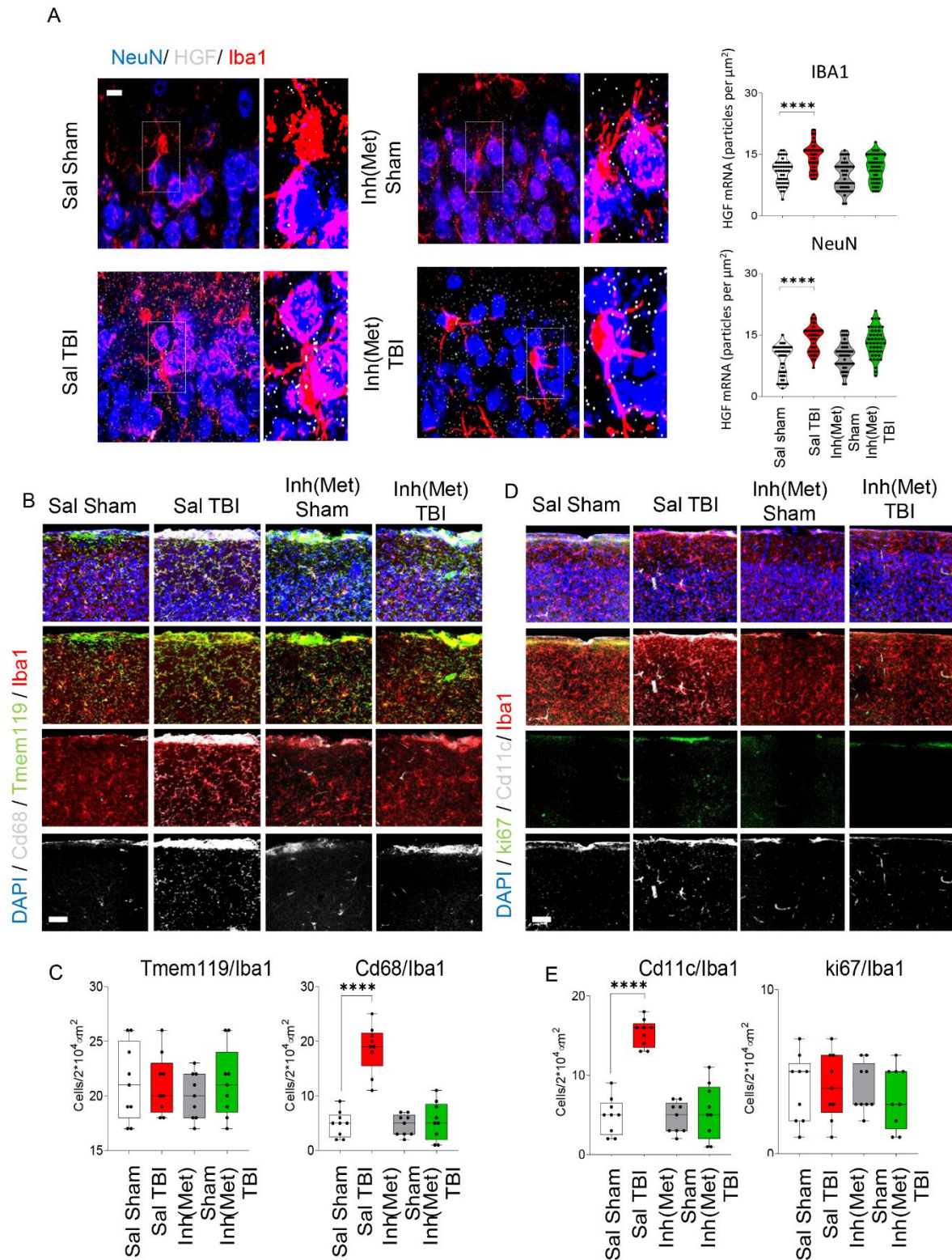


**Figure S4. Met inhibitor administered post- trauma does not affect HGF induction but prevents the phagocytic and disease-related microglia phenotype. Related to figure 4.**

**(A)** At 3h post injury, single-molecule in situ hybridization showed that HGF mRNA levels were significantly increased in both neurons and microglia after trauma. These levels, however, remained unaffected by inhibitor treatment. Small black dots indicate intensity of individual cells, green square the average per mouse; statistical analysis was performed on the average per mouse. Note that the representative images here correspond to the images reported in Fig. 4E; in this experiment, in situ for C3 and HGF was performed with distinct probes, together with Iba1 and NeuN immunostaining. The same image is shown to highlight that cells with C3 expression also show HGF expression. N=3/group, \* $p<0.05$ , \*\* $p<0.05$ , \*\*\* $p<0.0001$ . Scale bar: 10 $\mu$ m.

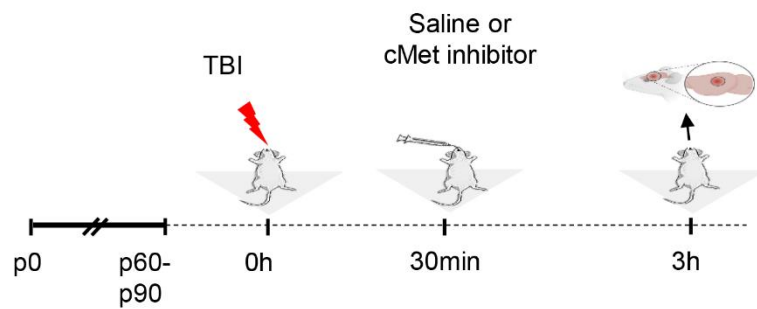
**(B-C)** Microglia specific marker Tmem119 and disease associated Cd11c were co-immunolabelled with Iba1 marker to explore microglia profile. No differences were observed in Tmem119+ Iba1+ cells among any group. At 3h post injury, Cd11c+Iba+ cells were increased and restored to normal levels after inhibitor treatment.

**(D-E)** Co-immunostaining with phagocytic marker CD68 and proliferating marker Ki-67 showed significant increase in the Cd68+ Iba1+ cells after trauma and reduced after inhibiting Met. However, no differences were observed in Ki-67+Iba1+ cells across all groups. Boxplots represent the 25-75 percentile (whiskers represent range); small dots represent individual sections, large green dots the average per animal; statistical analysis is performed considering individual animals as the biological unit. \* $p<0.05$ , \*\* $p<0.05$ , \*\*\* $p<0.0001$ . Scale bar: 300 $\mu$ m.

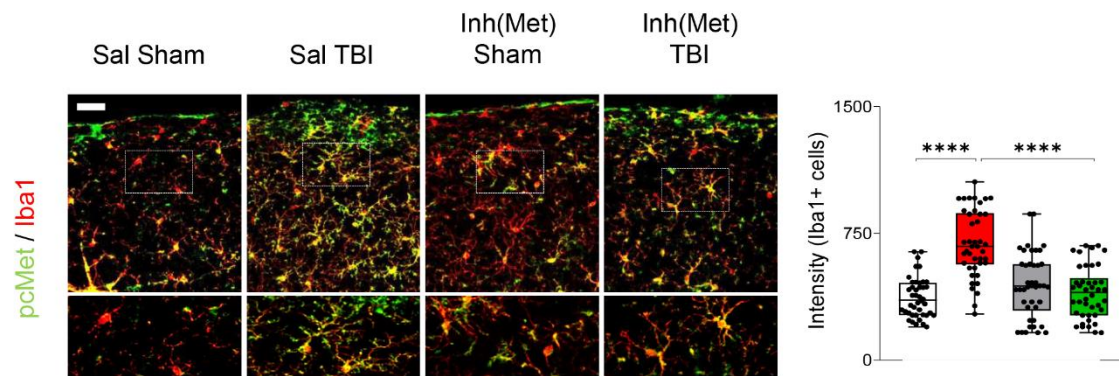


**Figure S5 Administration of the the Met inhibitor post-trauma still reduces microglial signaling and neuronal stress. Related to figure 5.**

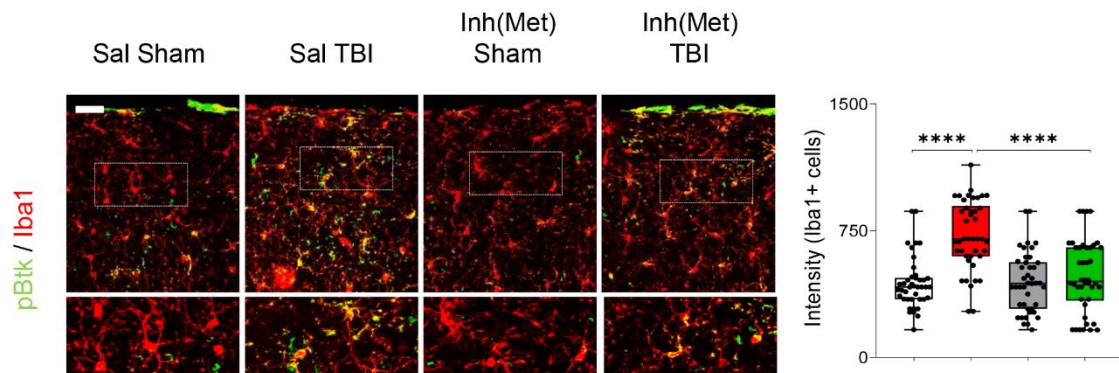
A



B



C



D

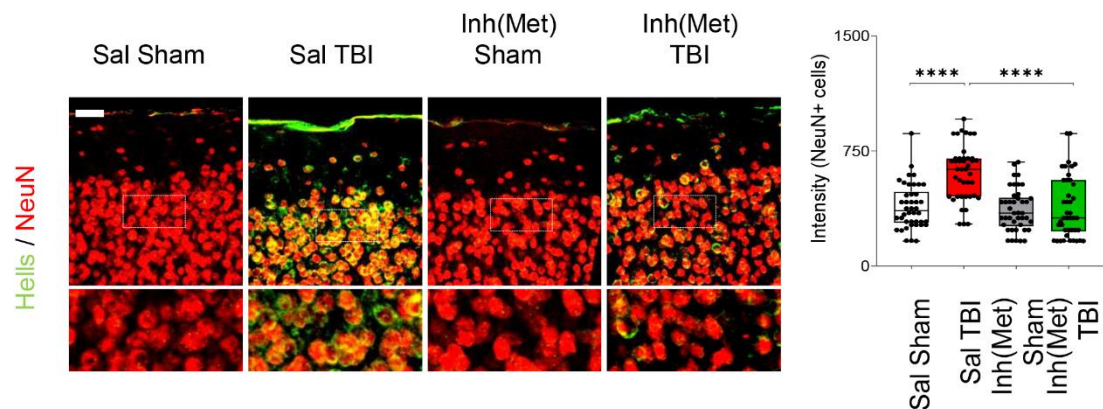
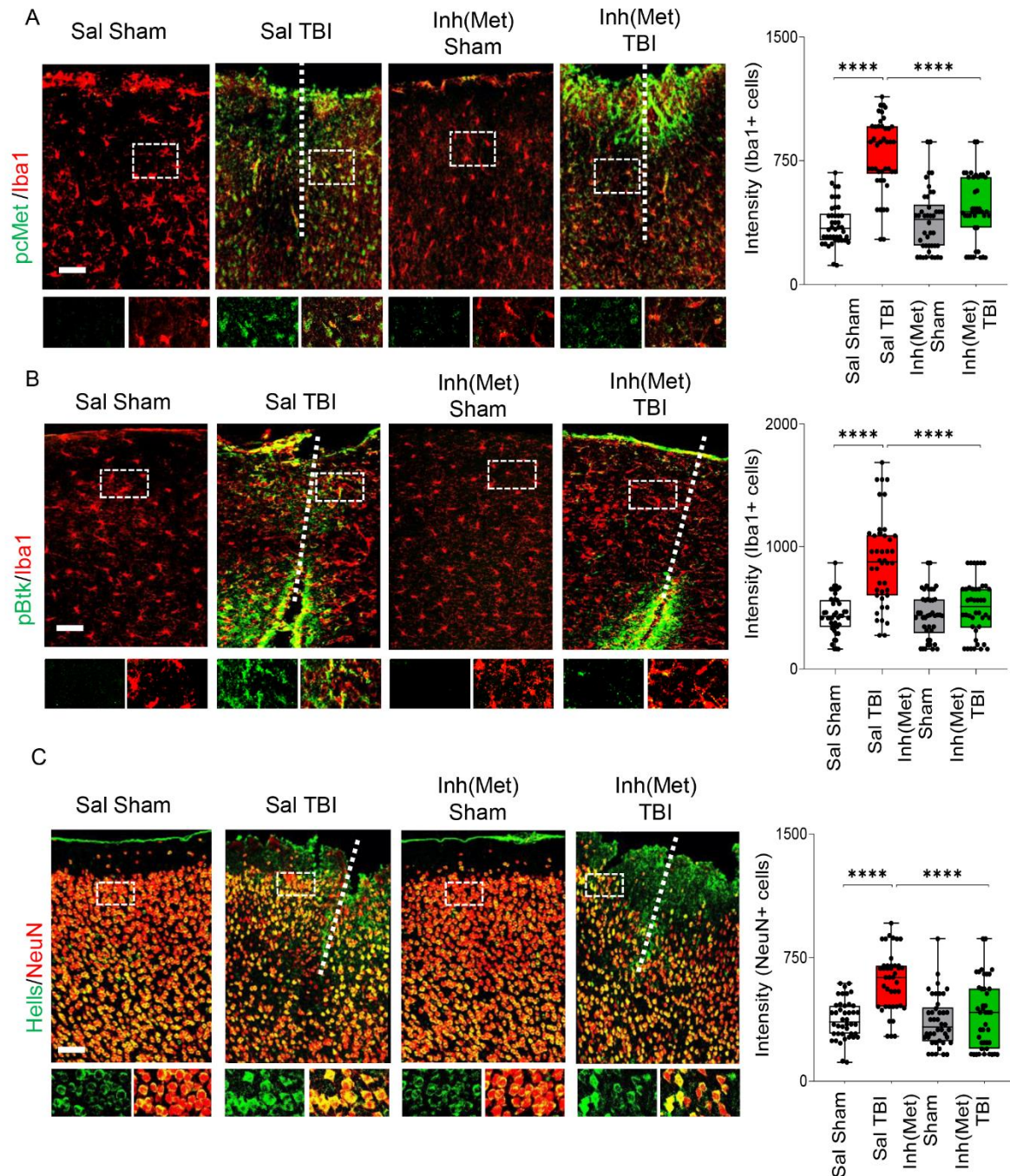


**Figure S5. Administration of the the Met inhibitor post-trauma still reduces microglial signaling and neuronal stress. Related to figure 5**

**(A)** Schematic outline of the experiment. Mice were subjected to TBI and either saline or Met inhibitor was administered after 30 mins and samples were collected at 3h post injury. **(B-C)** Immunostaining of pMet and pBtk showed significant upregulation in Iba1+ microglia cells post TBI and reduced upon inhibitor treatment. **(D)** The intensity levels of Hells were significantly upregulated 3h post trauma whereas reduced to baseline levels upon inhibitor treatment. Boxplots represent the 25-75 percentile (whiskers represent range); small dots represent individual sections, large green dots the average per animal; statistical analysis is performed considering individual animals as the biological unit. N=3/group, \* $p<0.05$ , \*\* $p<0.05$ , \*\*\* $p<0.0001$ . Scale bars: 200 $\mu$ m

**Figure S6. Blockade of Met reduces microglial signaling and neuronal stress also in the Stab Wound Injury (SWI) model. Related to figure 5.**



**Figures S6. Blockade of Met reduces microglial signaling and neuronal stress also in the Stab Wound Injury (SWI) model. Related to figure 5.**

**(A-B)** Immunostaining of pMet and pBtk showing significant upregulation in Iba1+ microglia cells post TBI and reduced upon inhibitor treatment 3h after SWI. **(C)** The intensity levels of Hells were significantly upregulated 3h post SWI whereas reduced to baseline levels upon inhibitor treatment. Boxplots represent the 25-75 percentile (whiskers represent range); small dots represent individual sections, large green dots the average per animal; statistical analysis is performed considering individual animals as the biological unit. N=3/group, \* $p < 0.05$ , \*\* $p < 0.05$ , \*\*\* $p < 0.0001$ . Scale bar: 250 $\mu$ m



**Figure S7. Met inhibitor elicits beneficial acute and longer-term effects on microglial morphology. Related to figure 6.**

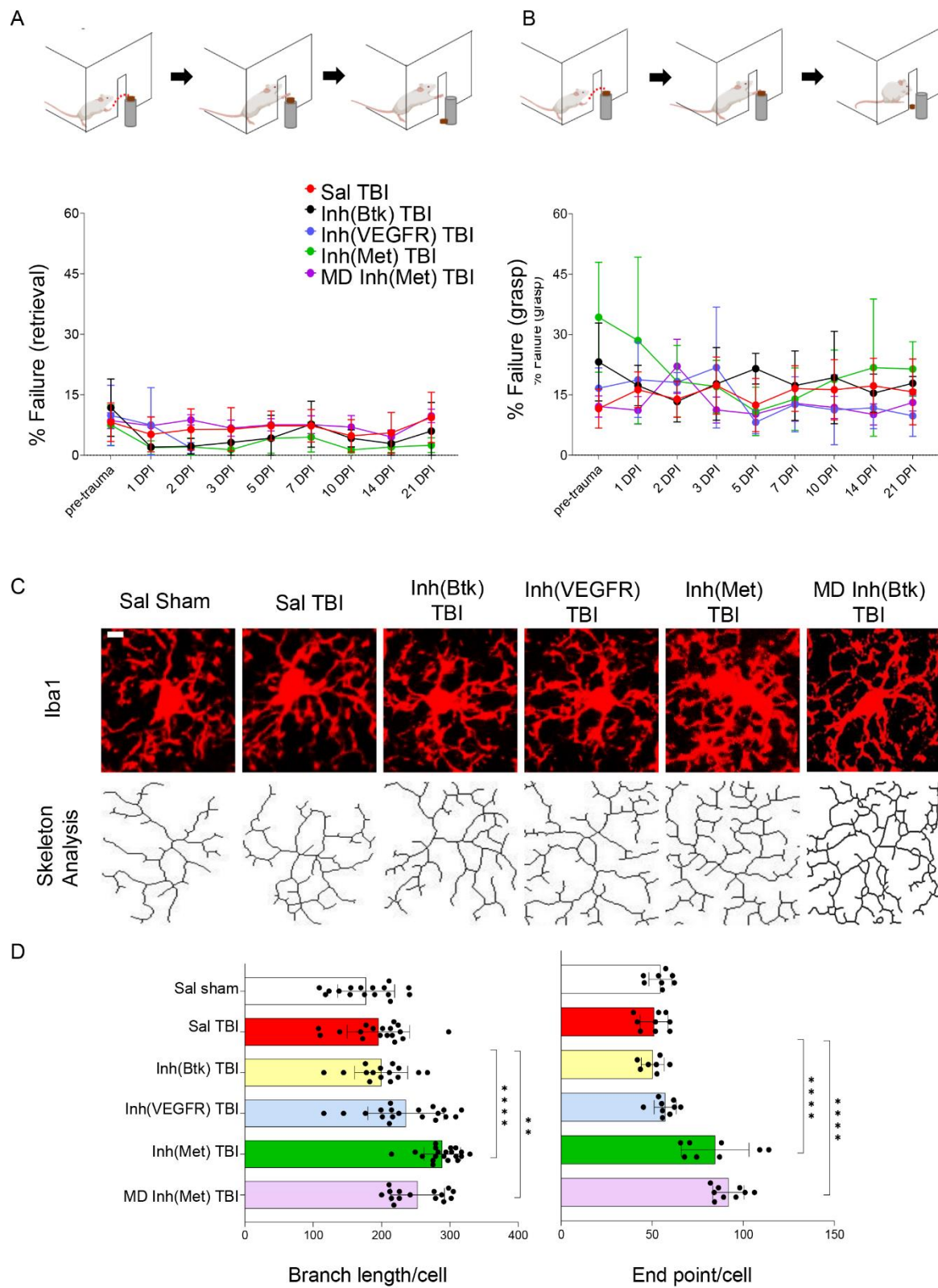


**Figure S7. Met inhibitor elicits beneficial acute and longer-term effects on microglial morphology. Related to figure 6.**

**(A-B)** The results showed failures in retrieval (underscoring digit control impairment) and grasping (underscoring the impairment in digit movements) among five treatment groups. No significant changes or patterns were observed among the groups. **(C-D)** Morphological changes in microglia showed increase in branch length and endpoints/cell upon single or multiple doses of Met inhibitor treatment displaying a ramified or arborized microglia morphology.

All graphs were represented as mean  $\pm$  SD. In **(A-D)**, n=7 for Sal TBI, n=3 for Inh(Btk) TBI, n=4 for Inh(VEGFR) TBI and Inh(Met) TBI, and n=6 for MD Inh(Met) TBI. small dots represent individual sections, large green dots the average per animal; statistical analysis is performed considering individual animals as the biological unit by Two-way ANOVA with Tukey correction. (\*P<0.05, \*\*P<0.001, \*\*\*P<0.001, \*\*\*\*P<0.0001). Scale bar: 10 $\mu$ m



**Table S5.** Clinico-demographic information of human patients (TBI and controls) for whom HGF levels were determined in CSF samples (Related to Figure 7).

<b>Data information</b>	<b>Control group*</b>	<b>Control group* 2</b>	<b>D0 group</b>	<b>longitudinal group</b>
N (M/F)	6 (2/4)	13 (7/6)	28 (21/7)	11 (7/4)
Age (median, range)	71 (53-85)	32.5(25-40)	34.5 (21-55)	29 (23-42)
Glasgow Coma Scale (median, range)	N/A	N/A	6 (3-9)	6 (3-7)
Injury Severity Score (median, range)	N/A	N/A	34.5 (17-59)	43 (17-59)
Glasgow Outcome Scale-Extended (median, range)	N/A	N/A	4 (1-8)	4 (1-6)

\* non-TBI CSF samples were obtained from patients with normal pressure hydrocephalus control group 1 and younger patients with tension-type headache-control group 2.